



Contents lists available at ScienceDirect

## Earth and Planetary Science Letters

journal homepage: [www.elsevier.com/locate/epsl](http://www.elsevier.com/locate/epsl)

# Evidence for rapid geomagnetic field intensity variations in Western Europe over the past 800 years from new French archeointensity data

Agnès Genevey<sup>a,\*</sup>, Yves Gallet<sup>b</sup>, Jean Rosen<sup>c</sup>, Maxime Le Goff<sup>b</sup>

<sup>a</sup> Centre de Recherche et de Restauration des Musées de France, UMR CNRS 171, Palais du Louvre, Porte des Lions, 14 quai F. Mitterrand, 75001 Paris, France

<sup>b</sup> Equipe de Paléomagnétisme, Institut de Physique du Globe de Paris, UMR CNRS 7154, 4 place Jussieu, 75005, Paris, France

<sup>c</sup> UMR CNRS 5594, ARTEHIS, Faculté des Sciences, 6 Bd Gabriel, 21000 Dijon, France

## ARTICLE INFO

## Article history:

Received 22 December 2008

Received in revised form 7 April 2009

Accepted 15 April 2009

Available online xxx

Editor: T. Spohn

## Keywords:

archeomagnetism  
 archeointensity  
 secular variation  
 past millennium  
 Western Europe  
 dipole moment

## ABSTRACT

The number of reliable archeointensity determinations obtained from Western Europe for the past millennium remains limited. Moreover, the large scatter between different datasets available is puzzling. The present study analyzed 31 new groups of baked clay (ceramic or brick) fragments sampled in France (29 groups) and in Belgium (2 groups). These groups contain several fragments collected from different artefacts and are precisely dated principally from historical constraints between the XIIIth and the XIXth centuries. Additionally, we re-evaluated 14 intensity values that we previously obtained from the same time period. The fragments were analyzed using two different thermal methods: (1) the “in field-zero field” (IZ) or the IZZI version of the classical Thellier and Thellier method and (2) the Triaxe protocol that involves high-temperature magnetization measurements. Data were corrected for the anisotropy of thermoremanent magnetization (TRM) and the dependence of TRM acquisition on the cooling rate was taken into account in the different protocols. Archeointensity data obtained on twin specimens sampled from the same fragment and using both experimental techniques generally show a good agreement (i.e. within 5%) at the fragment and at the site level. All retained site-level averaged intensity results (43 of 45 groups) have standard deviations of less than 5  $\mu\text{T}$ . Furthermore, groups of approximately the same age have very consistent archeointensity. Altogether, the data presented herein recover a detailed and smoothed geomagnetic field intensity variation curve characterized by two peaks in intensity, the first during the second half of the XIVth century and the second around AD 1600, followed by a significant decreasing trend in intensity during most the XVIIth and XVIIIth centuries. This evolution does not satisfactorily fit with the expected intensity values for France derived from geomagnetic field models relying on a different evolution of the axial dipole moment. Our results lead us to propose that the axial dipole moment decreased from AD 1600 to the end of the XVIIIth century, then slightly increased up to ~AD 1850 before decreasing again to present day.

© 2009 Elsevier B.V. All rights reserved.

## 1. Introduction

Since the pioneering work of Emile Thellier in the late 30s, our knowledge of the secular variation of the Earth's magnetic field in Western Europe over the last three millennia has benefited from numerous archeomagnetic studies, whose number has greatly increased in the past few years (e.g. Gómez-Paccard et al., 2006a; Tema et al., 2006; Zanani et al., 2007). Most of these studies however have focused on the determination of ancient geomagnetic directions. In France, the analysis of numerous well dated in-situ burned structures, such as pottery and domestic kilns, has allowed us to recover in detail the regional directional variations (Thellier, 1981; Bucur, 1994; Gallet et al., 2002). Thanks to its high precision, the resulting curve is currently used as a dating tool in archeology to date in-situ structures of unknown age (e.g. Lanos et al., 1999; Le Goff et al., 2002). Much of this archeomagnetic

dating was, for instance, performed on French domestic kilns of the early Middle Ages (roughly between the Vth and the Xth century AD), a ‘favorable’ period characterized by rather large changes in magnetic direction (e.g. Warmé, 2005).

In contrast, the number of reliable archeointensity determinations obtained from Western Europe is still limited. As a consequence, the variations in geomagnetic field intensity are not well known for this area and the occurrence of several features in intensity behavior suggested in the literature is presently debated (e.g. Genevey and Gallet, 2002; Gallet et al., 2005; Gómez-Paccard et al., 2006b, 2008). New archeointensity data is thus necessary in order to reconstruct the full vector evolution (direction and intensity) of the geomagnetic field over the past few millennia. This is a particularly important objective as several authors recently suggested a causal link between these variations and atmospheric processes (and climate) over multi-decadal and centennial scales (e.g. Gallet et al., 2005, 2006; Usoskin et al., 2008; Gallet et al., in press). In addition, similarly to the magnetic directions, the intensity variations appear as a very promising dating tool for archeologists and museum

\* Corresponding author.

E-mail address: [agnes.genevey@culture.fr](mailto:agnes.genevey@culture.fr) (A. Genevey).

curators as it would allow the dating of displaced objects (i.e. from their original location of firing), such as ceramics, tiles or bricks. The efficiency of this method would however rely on the occurrence of rapid intensity fluctuations and on our ability to obtain reliable intensity values. Considering the dispersion of the intensity data observed in some regions or between different datasets (e.g. Genevey et al., 2008), this latter point is clearly not trivial. In particular, the data scatter led Gómez-Paccard et al. (2006b, 2008) to conclude that the uncertainties attached to the intensity results are too large to allow the identification of the rapid fluctuations previously proposed between the XIIIth and the XIXth century in France by Genevey and Gallet (2002) and Gallet et al. (2005).

In this debate, which therefore addresses both the reality of rapid regional intensity variations and the reliability of the archeointensity determinations, the past millennium in Western Europe appears as a very suitable target. Sampling opportunities are indeed numerous for this time interval but more importantly, some archeological and historical research conducted on archive documents make it possible to select very well dated groups of fragments. In this study, we will see that the age uncertainties can be sometimes as low as a year or a few years. Thus, following on from our previous studies (Genevey and Gallet, 2002; Gallet et al., 2005), we report here new archeointensity results precisely dated between the XIIIth and the XIXth centuries.

## 2. The archeological collection

Our archeological collection consists of 31 groups of baked clay fragments sampled in France apart from two from Belgium at Alost (Fig. 1, Table 1). Dated from the beginning of the XIIIth century to the middle of the XIXth century, this new collection follows the history of French faience from its appearance in Marseille (Sainte-Barbe workshop; Marchesi et al., 1997), through the ornamental bricks at Longecourt-en-Plaine, (first known case of faience for the Renaissance period in 1495; Fig. 2a; Rosen, 2000), to the early faience industry, illustrated notably by

the Nevers pottery (Rosen and Crépin-Leblond, 2000; Rosen, 2001). The term “faience” refers to a type of pottery covered in glaze containing tin oxide which gives a white and opaque aspect to the ceramic closely resembling the texture of porcelain (Fig. 2a,b). Its manufacturing process consists of at least two heating phases, first to bake the clay without glaze to obtain the so-called “biscuits” (Fig. 2c) then to vitrify the glazing blend applied on the biscuit. Our different groups exemplify the various materials involved in the faience production, including fragments from kilns where the pottery was originally baked, potsherds from the biscuits or from the final faience and fragments of baked clay tools used to separate the decorated pottery. Apart from these faience materials, a few other groups of baked clay fragments complete our collection. This is for instance the case of the PALO2 group. The fragments of this set were discovered during the excavations of the Grand Louvre in Paris at the end of the 1980s. They were originally manufactured during the third part of the XVIth century to be part of a grotto constructed by Bernard Palissy, a famous French potter from the Renaissance, to decorate the Tuileries garden for Queen Catherine de Médicis.

Each of our groups corresponds to an archeological unit as specified by archeologists and museum curators. It may be, for example, a stratigraphic layer identified during the excavations of a site. It can also be defined based on the typomorphological characteristics of the potsherds or may simply correspond to a collection of bricks produced for a specific pavement (Table 1 in the Appendix). Several sets, differentiated on the basis of the archeological description, are however associated to the same period of use of a kiln in a pottery workshop and should be therefore considered together for deriving a mean intensity. The groups LYON01/A, /B, /C sampled from three different stratigraphic units identified during the excavations are for instance all associated with the Joseph Combe faience workshop whose period of activity was found to be very short [1732–1734] according to documentary sources. Altogether our collection is therefore composed of 24 new main groups with distinct ages (Table 1).

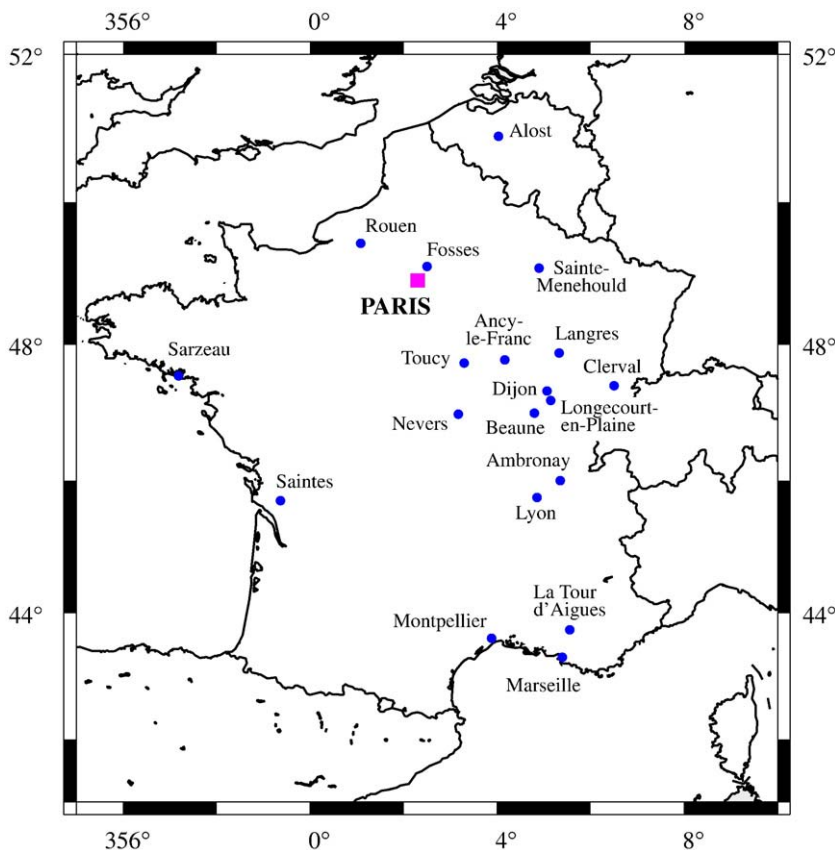


Fig. 1. Location map of the sites where the collected pottery, bricks and baked clay fragments were originally produced.

**Table 1**

New archeointensity data obtained from 43 groups of pottery and brick fragments sampled in France (41 groups) and in Belgium (2 groups).

Archeomagnetic Label	Status	Site	Lat (°N)	Long (°E)	Age (AD)	Type of material	Intensity Method(s)	N Fragment	n Specimen	Fmean ± oF (μT)	Fmean in Paris (μT)
A07	PS (a)	Fosses	49.1	2.5	1200–1250	Potsherd	TT-IZ and Triaxe	6	14	53.8 ± 4.1	53.7
MAR02	N	Marseille	43.3	5.4	1225–1250	Potsherd	Triaxe	5	5	50.4 ± 3.4	53.4
A08	PS (a)	Fosses	49.1	2.5	1250–1300	Potsherd	TT-IZ and Triaxe	7	14	54.7 ± 2.6	54.6
A11	PS (a)	Fosses	49.1	2.5	1300–1350	Potsherd	TT-IZ and Triaxe	5	12	52.0 ± 3.0	51.9
FSAR	N	Ambronnay	46.0	5.4	1323–1330	Brick from Hearth	Triaxe	3	3	54.7 ± 1.4	56.3
HDM01	N	Paris	48.9	2.3	1325–1350	Potsherd	Triaxe	3	6	55.1 ± 2.6	55.1
SUSC02	N	Sarzeau	47.5	−2.8	1330–1350	Pavement Brick	Triaxe	6	6	57.9 ± 1.7	58.7
ALOST01	N	Alost	50.9	4.0	1360	Potsherd	Triaxe	4	4	60.4 ± 3.4	59.3
A12	PS (a)	Fosses	49.1	2.5	1350–1400	Potsherd	TT-IZ and Triaxe	6	10	57.1 ± 1.4	57.0
A13	N	Fosses	49.1	2.5	1400–1450	Potsherd	Triaxe	3	4	54.3 ± 1.1	54.2
HB01	N	Beaune	47.0	4.8	1448–1452	Pavement Brick	Triaxe	5	8	51.0 ± 2.1	52.0
ALOST03	N	Alost	50.9	4.0	1475–1498	Potsherd	TT-IZZI	3	6	50.4 ± 2.2	49.5
LONG01	N	Longecourt-en-Plaine	47.2	5.2	1495	Pavement Brick	Triaxe	6	6	50.7 ± 1.6	51.6
LYON02	N	Lyon	45.8	4.9	1510–1540	Potsherd	TT-IZZI and Triaxe	6	13	48.6 ± 4.4	50.1
A16	PS (a)	Fosses	49.1	2.5	1500–1550	Potsherd	TT-IZ and Triaxe	5	15	52.7 ± 3.2	52.6
PAR01	N	Paris	48.9	2.3	1530–1540	Potsherd	TT-IZZI	3	6	53.4 ± 1.9	53.4
EC01	N	Rouen	49.4	1.1	1542	Pavement Brick	TT-IZZI and Triaxe	4	10	52.6 ± 2.1	52.3
EC02	N	Rouen	49.4	1.1	1549–1551	Pavement Brick	TT-IZZI and Triaxe	5	14	53.3 ± 3.2	53.0
LAN01	N	Langres	47.9	5.3	1551	Pavement Brick	Triaxe	8	8	52.7 ± 1.2	53.2
A22	N	Fosses	49.1	2.5	1550–1570	Potsherd	Triaxe	5	5	52.5 ± 0.9	52.4
PAL02	N	Paris	48.9	2.3	1550–1572	Baked Clay	TT-IZZI	2	4		52.4 ± 2.1
		Saintes	45.7	−0.6				1	2		
A18	PS (a)	Fosses	49.1	2.5	1550–1600	Potsherd	TT-IZ and Triaxe	5	13	X	X
TA01	N	La Tour-d'Aigues	43.7	5.6	1570–1584	Pavement Brick	TT-IZZI and Triaxe	5	11	53.6 ± 4.1	56.5
CL01	N	Clerval	47.4	6.5	1610–1625	Potsherd	TT-IZZI and Triaxe	5	11	52.1 ± 1.5	52.9
MON03	PS (b)	Montpellier	43.6	3.9	1614–1679	Potsherd	TT-IZZI and Triaxe	5	9	51.4 ± 2.2	54.3
MON01	PS (b)	Montpellier	43.6	3.9	1614–1679	Potsherd	TT-IZZI and Triaxe	5	8	51.4 ± 1.3	54.3
MON07	N	Montpellier	43.6	3.9	1614–1679	Potsherd	Triaxe	2	2	51.9 ± 1.0	54.8
MON08	N	Montpellier	43.6	3.9	1614–1679	Baked Clay (from Kiln)	TT-IZZI and Triaxe	5	11	52.1 ± 3.0	55.0
MON01 + MON07 + MON08 *		Montpellier	43.6	3.9	1614–1679	Baked Clay (from Kiln) and Potsherd	TT-IZZI and Triaxe	12	21	51.8 ± 2.0	54.7
MON04	N	Montpellier	43.6	3.9	1614–1679	Potsherd	TT-IZZI and Triaxe	5	7	49.6 ± 0.6	52.4
MON05	N	Montpellier	43.6	3.9	1614–1679	Potsherd	Triaxe	2	2	51.7 ± 0.8	54.6
MON04 + MON05 *	N	Montpellier	43.6	3.9	1614–1679	Potsherd	TT-IZZI and Triaxe	7	9	50.2 ± 1.2	53.0
NE02	PS (b)	Nevers	47.0	3.2	1660–1680	Potsherd	TT-IZZI and Triaxe	4	6	45.5 ± 2.0	46.4
MON02	N	Montpellier	43.6	3.9	1660–1692	Potsherd	Triaxe	4	4	48.7 ± 3.4	51.4
NE04	PS (b)	Nevers	47.0	3.2	1720–1735	Potsherd	TT-IZZI and Triaxe	1	3	X	X
LYON01/A	N	Lyon	45.8	4.9	1732–1733	Potsherd	TT-IZZI and Triaxe	8	17	43.8 ± 2.1	45.2
LYON01/B	N	Lyon	45.8	4.9	1732–1733	Potsherd	Triaxe	4	4	44.7 ± 2.2	46.1
LYON01/C	N	Lyon	45.8	4.9	1732–1733	Potsherd	Triaxe	5	5	44.3 ± 1.7	45.7
LYON01/A + B + C *	N	Lyon	45.8	4.9	1732–1733	Potsherd	TT-IZZI and Triaxe	17	26	44.2 ± 1.9	45.6
NE05	PS (b)	Nevers	47.0	3.2	1760–1780	Potsherd	TT-IZZI and Triaxe	8	11	43.2 ± 2.3	44.0
ALF01/02	N	Ancy-le-Franc	47.8	4.2	1770–1780	Potsherd	Triaxe	11	11	42.9 ± 2.1	43.4
BDE01	N	Sainte-Menehould	49.1	4.9	1785–1815	Potsherd	Triaxe	7	7	44.2 ± 1.0	44.1
BDE02	N	Sainte-Menehould	49.1	4.9	1785–1815	Potsherd	Triaxe	3	3	43.9 ± 1.3	43.8
BDE01 + 02 *	N	Sainte-Menehould	49.1	4.9	1785–1815	Potsherd	Triaxe	10	10	44.1 ± 1.0	44.0
ALF03	N	Ancy-le-Franc	47.8	4.2	1797–1807	Potsherd	Triaxe	7	7	44.1 ± 1.3	44.6
ART02	N	Toucy	47.7	3.3	1819–1846	Baked Clay Tool	Triaxe	2	2	44.9 ± 0.1	45.4
ART03	N	Toucy	47.7	3.3	1819–1846	Potsherd	Triaxe	2	2	43.6 ± 2.1	44.1
ART02 + ART03 *	N	Toucy	47.7	3.3	1819–1846	Baked Clay Tool and Potsherd	Triaxe	4	4	44.2 ± 1.8	44.7
NE06	PS (b)	Nevers	47.0	3.2	1818–1848	Potsherd	TT-IZZI and Triaxe	3	6	43.8 ± 0.1	44.6
NE07	PS (b)	Dijon	47.3	5.0	1845–1855	Potsherd	TT-IZZI and Triaxe	5	11	45.3 ± 2.6	46.0

The label in the "Status" column allows one to distinguish between (N) New groups of fragments analyzed in the present study and groups Previously Studied (PS) in (a) Genevey and Gallet (2002) or (b) Gallet et al. (2005) for which we re-evaluated here the intensity means. N fragment, number of different fragments retained per group for computing a mean intensity value; n specimen, total number of specimens analyzed and retained per group; Fmean ± oF, mean intensity at group-level and standard deviation in μT; F<sub>mean in Paris</sub>, mean intensity reduced to the latitude of Paris (48.9°N). The crosses in the "results" columns indicate that no intensity mean were retained for the two corresponding groups (A18 and NE04). The A18 group was rejected because of a negative comparison test between the results derived using the Triaxe and TT-IZ protocols. For group NE04, only one TT-IZZI result passed a selection criteria relative to the coherence between the IZ and ZI slopes (see the text for further explanation). The "\*" in the archeomagnetic label column highlights the cases for which two or three "regular" groups of fragments associated to the same period of activity of a kiln were analyzed. A "master" mean value was then computed in each case. For complete table (with archeological descriptions and dating constraints), see Table 1 in the Appendix.

Special care was paid while building up this collection to select only well dated groups of artifacts. The uncertainty in age is generally less than 30 years (in any case less than 65 years) and the dating relies on several arguments, often combined, as archeological constraints (e.g. stratigraphy, typomorphology of the ceramic, coins...) and/or historical documents, and/or inscriptions (Table 1 in the Appendix). In several cases, the age precision is to within a year or a few years. The HB01 group (Fig. 2d) corresponding to the pavement

of the so-called King's room in the Hospices de Beaune is for example precisely dated to 1448–1452 from archives. As indicated in rediscovered historical documents, the order for this pavement was indeed made in March 1448 and the first patient was welcomed in the hospital at the beginning of 1452. For the pavement bricks of the cathedral's chapel in Langres (Fig. 2b), the dating is also remarkably precise, resulting from a direct inscription engraved on the ceiling of the chapel.

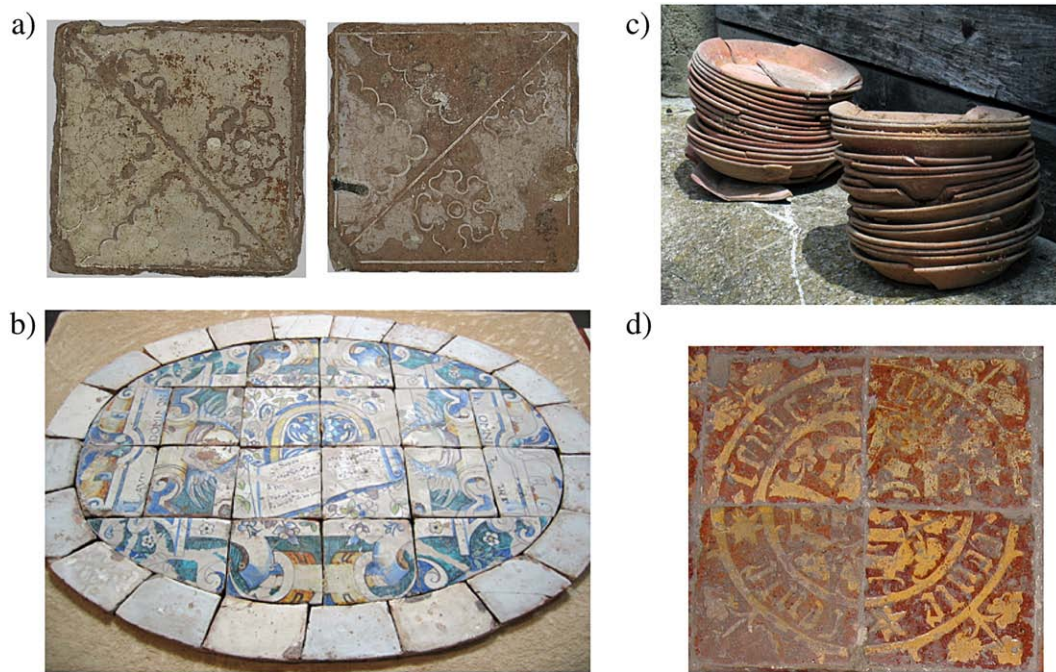


**Fig. 2.** Examples of archeological artifacts analyzed. (a) Two tin-glazed pavement bricks with a monochrome “décor” collected at the Longecourt castle (group LONG01) © Daniel Vigears, C2RMF (b) Pavement's unit of the chapel of the cathedral of Langres (Museum of Langres). The fragments analyzed (LAN01) are from bricks similar to the monochrome white tin-glazed tiles © Agnès Genevey, C2RMF. (c) Fragment of plates without glazed (“Biscuits”) discovered inside kiln #1 of the Ancy-le-Franc workshop (group ALF3) © Agnès Genevey, C2RMF (d) Pavement of the Hospices de Beaune - Detail of four bricks. © Agnès Genevey, C2RMF.

Fourteen groups from Fosses, Montpellier and Nevers previously studied in Genevey and Gallet (2002) and Gallet et al. (2005) are also included in the present paper as new or/and old fragments were since then (re)-analyzed using a different intensity protocol (Table 1). Note that for both the MON03 and MON01 sites from Montpellier, a larger age uncertainty is now retained as we chose to exclude any constraints from archeomagnetism (i.e. from magnetic directions) to rely, as for all our other sites, only on independent archeological and historical arguments.

### 3. Intensity experiments

Prior to the intensity experiments, we investigated for all fragments from our new collection the temperature variations of their low-field magnetic susceptibility using a KLY-3 kappabridge apparatus with a CS3 temperature control unit. Heating-cooling cycles were performed between 20 °C and 550 °C to test the stability of the magnetic mineralogy within the temperature range used for the intensity determinations. Here, the reversibility of the cycles was used as a criteria to retain or reject the fragments (Fig. 3). The shape of the resulting curves significantly varies from site to site, and in a few cases within a site itself (see Fig. 3). These differences probably reflect variations in the composition of the clay, in the clay paste preparation and/or in the conditions of heating-cooling phases experienced by the archeological artifacts. For two selected fragments from each group, we also carried out measurements of isothermal remanent magnetization (IRM) acquisition and hysteresis loops using laboratory-built instruments. The saturation of IRM is generally reached in a field weaker than 0.3T, and the hysteresis parameters for those fragments fall in the pseudo-single domain region of magnetite (Day et al., 1977). In a few fragments, however, a high-coercivity magnetic phase is also detected as their magnetization is still not saturated in a field of 0.8T (Fig. 4). These fragments exhibit wasp-waisted hysteresis loops likely induced by the presence of both magnetite and hematite, the latter phase being also deduced from the thermal demagnetization of the concerned fragments.

At this step, the unstable behavior observed in the magnetic mineralogy for several fragments led to the rejection of a few sites. Note that in part 2 we only described the sites retained for further archeointensity experiments.

Two experimental protocols were used for the intensity determinations. They both derive from the Thellier and Thellier (1959) method which relies on the replacement of the original natural remanent magnetization (NRM) of the fragments (supposed to be a pure TRM) by a new TRM acquired in a laboratory field of known direction and intensity.

#### 3.1. TT-IZZI procedure

The first protocol follows the so-called IZZI procedure (Yu et al., 2004). It involves a succession, with increasing temperature, of double heating-cooling steps (In field-Zero field) (or IZ) then (Zero Field-In Field) (or ZI), the “Zero Field” steps corresponding to the partial demagnetization of the NRM and the “In Field” steps to the acquisition of a partial TRM (pTRM). The TT-IZZI protocol was designed that way to allow the detection of multi-domain grains behavior and to benefit from the advantages of both Coe's (1967) and Aitken's (e.g. Aitken et al., 1988) version of the Thellier and Thellier method (Yu et al., 2004).

For each fragment analyzed using this protocol, we prepared three specimens with a square base of 1 cm<sup>2</sup> and a height depending on the thickness of the fragments but in any case less than 1 cm. Two specimens were dedicated to the intensity experiments and the last one was prepared for the cooling rate experiments.

The TT-IZZI intensity experiments were performed on two series of specimens with for the first one, 13 double heating steps from 150 °C to 500 °C. For the second set, 19 double heating-cooling steps were included from 100 °C to 575 °C. Temperature intervals were of 50 °C until 200 °C and 150 °C for respectively the first and second series then of 25 °C in both cases.

After each (In field-Zero field) step, i.e. every two temperature steps, a partial TRM was additionally acquired at a lower temperature in order to test the stability of the TRM acquisition capacity.

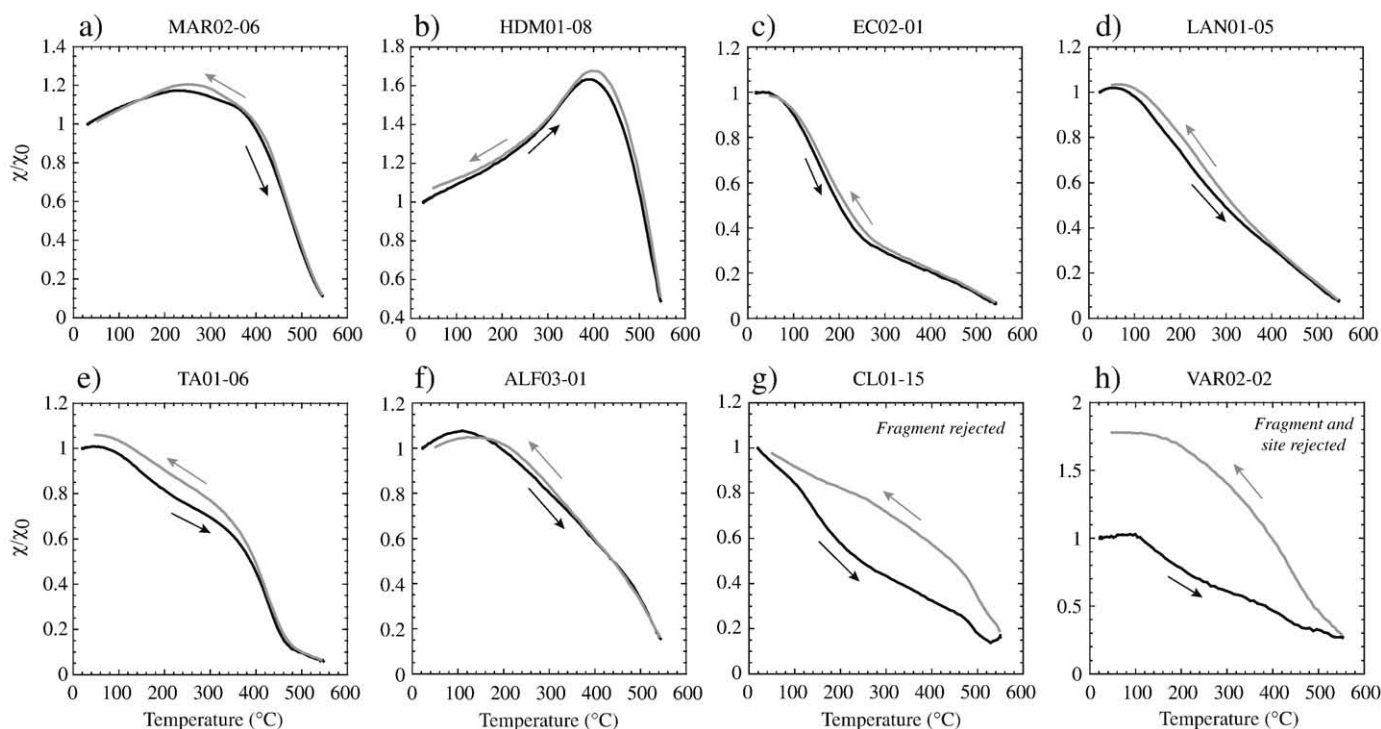


**Fig. 3.** Normalized bulk susceptibility versus temperature curves obtained for different fragments. (a) to (f) Examples of favorable behavior for archeointensity determinations. (g, h) Two examples of rejected fragments because of magnetic alteration during heating.

Experiments were carried out in air and the laboratory field was applied both during the heating and the cooling of the specimens parallel to their  $x$  axis. The coordinates system is arbitrary but was set in such way that the  $x$  axis is in the stretching plane of the pottery. Note further that for each pair of specimens analyzed in intensity, the  $x$  axes were chosen to be perpendicular to each other to test our ability to reliably determine the TRM anisotropy tensor (see below). After each step, the measurements were made at ambient temperature using a 2G cryogenic magnetometer with a horizontal access housed in the shielded room of the paleomagnetic laboratory of the Institut de Physique du Globe de Paris.

During the course of the TT-IZZI procedure, the TRM anisotropy tensor was fully determined at two intermediate temperatures, through the acquisition of a partial TRM in successively six different

directions ( $x$ ,  $-x$ ,  $y$ ,  $-y$ ,  $z$ ,  $-z$ ) relatively to the specimen's coordinates. This anisotropy is generally interpreted as linked to an easy plane of magnetization identical to the stretching plane of the clay during the manufacturing process (e.g., Rogers et al., 1979; Aitken et al., 1981). From the TRM tensor, an anisotropy correction factor was computed following Veitch et al. (1984) and the mean of the two factors obtained for the two temperatures of tensor determination was then applied to the raw intensity value. Note that this was justified as the differences observed between the two factors were in all cases less than 1.5% and, for 85% of the specimens, less than 0.5% (see also Genevey and Gallet, 2002).

The cooling rate effect on the TRM acquisition was also investigated for each fragment on a companion specimen following the procedure described in detail in Genevey and Gallet (2002); see also Chauvin et al. (2000). Briefly it relies on the comparison between the intensity of two partial TRMs acquired with a rapid cooling rate, the one used in routine during the intensity procedure (here about 30 min from 450 °C) and a slow cooling rate chosen to mimic the conditions prevailing during the original cooling of the artifacts. The fragments analyzed with the TT-IZZI protocol were all originally baked in large kilns and a slow cooling time of about 30 h from 450 °C was therefore considered for these experiments.

The selection criteria applied to only retain the most reliable data obtained using the TT-IZZI protocol are summarized in Table 2 in the Appendix. They are very similar to those applied in Genevey and Gallet (2002); see also Gallet et al. (2005). For the control of the magnetic alteration, we however chose to normalize the difference between the pTRM and the pTRM-check by the total TRM intensity as in Chauvin et al. (2000) and by the length of the hypotenuse of the NRM/pTRM data used in the slope calculation as defined in Selkin and Tauxe (2000). In both cases we set a limit of 5%. The Cumulated Difference RATIO (CDRAT) parameter which allows us to detect a progressive alteration was fixed to 9% as a cutoff value. Additionally we introduced two parameters not considered in Gallet et al. (2005) to detect possible bias due to the presence of multi domain grains. Two directions were computed using respectively only the ZI and the IZ steps in the

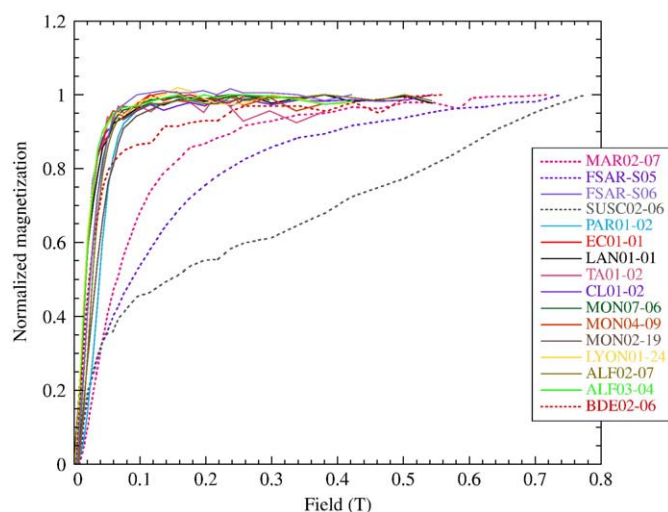


**Fig. 4.** Normalized IRM acquisition curves obtained for 16 representative pottery and brick fragments. (For interpretation of the references to color in this figure, the reader is referred to the web version of this article.)

thermal demagnetization diagram and similarly two slopes computed in the corresponding Arai diagram (Nagata et al., 1963). If no criterion was applied using the IZ and ZI directions – as the two directions were

always found to be very close (less than 2.5°) – we fixed a limit of 5% difference between the IZ and ZI slopes compared to the one computed using all the steps within the temperature interval chosen.

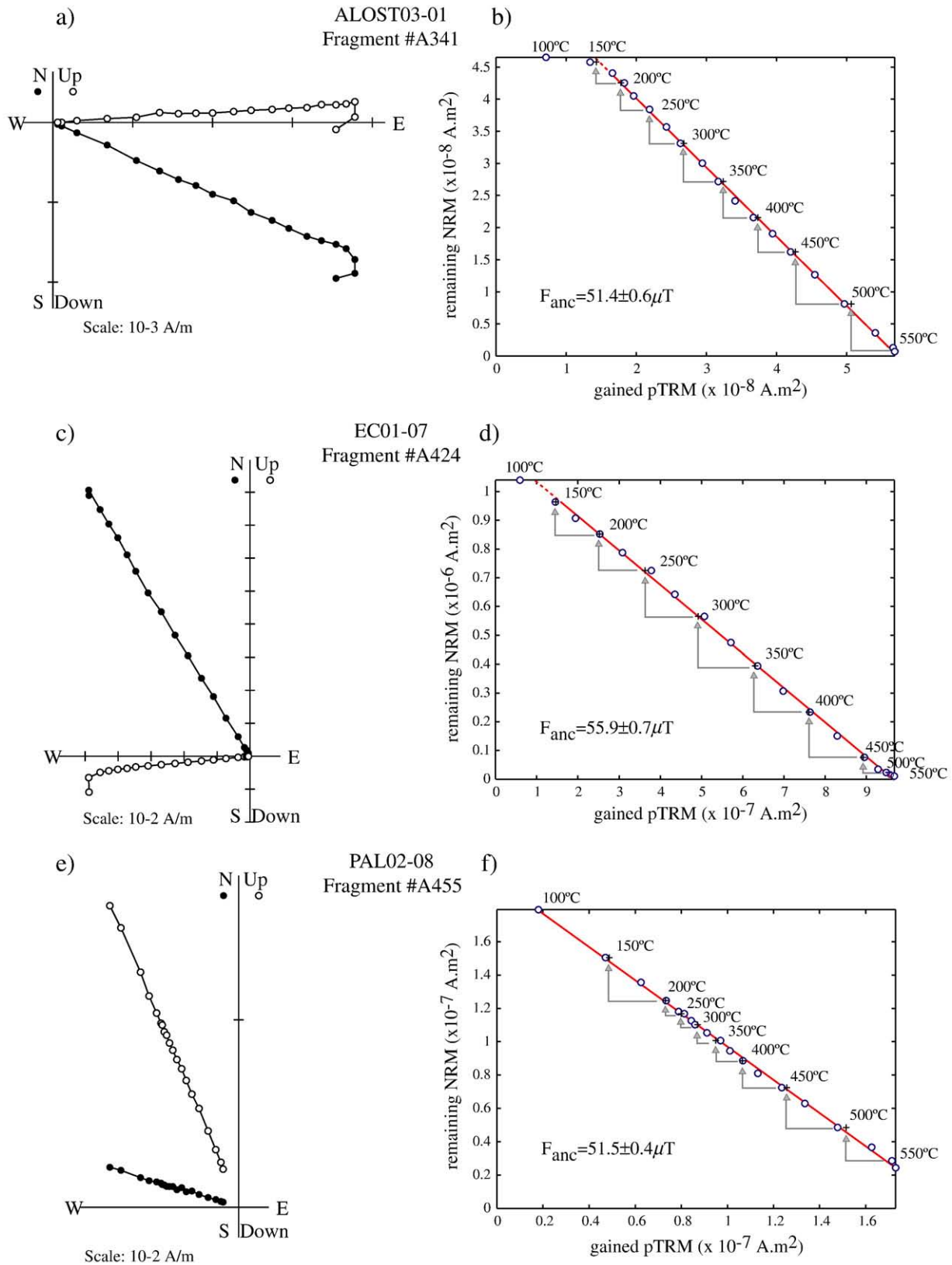


Fig. 5. Examples of thermal demagnetization diagrams (a, c, e) together with the corresponding remaining-NRM versus TRM-gained diagrams (b, d, f - open circles). In the demagnetization diagrams, the open (closed) symbols refer to the inclinations (declinations). During intensity experiments, pTRM-checks were performed every 2 thermal steps (crosses in b, d, f). The linear segments considered for slope computations are indicated by a continuous line.

### 3.2. Triaxe protocol

Intensity determinations were also carried out using a second procedure specially designed for the Triaxe equipment, hereafter named “Triaxe protocol”. The Triaxe is a three axis vibrating sample magnetometer developed at the paleomagnetic laboratory of the Institut de Physique du Globe de Paris (Le Goff and Gallet, 2004) that allows continuous magnetization measurements at high temperatures of each individual small core (1 cm-diameter, 1 cm-height). The Triaxe protocol which derives from the Thellier and Thellier method (1959) was fully described in Le Goff and Gallet (2004) and we only summarize below the main steps. It first implies the progressive and almost complete demagnetization of the NRM up to a relatively high temperature T2. The variations of the spontaneous magnetization ( $J_s$ ) between T1, usually equal to 150 °C, and T2 is next investigated in order to take into account the small magnetization fraction remaining blocked above T2. A TRM is then acquired by cooling the specimen between T2 and the low temperature T1 in a field whose direction is set parallel to the one of the NRM and the intensity chosen to be close to the expected one. The new TRM is finally continuously demagnetized between T1 and T2.

For each temperature  $T_i$  running from T1 to T2 with a step of  $\sim 5$  °C we compute the parameter  $R'(T_i)$  which is the ratio between the NRM and TRM fractions unblocked between T1 and  $T_i$  (both corrected for the thermal variations of the NRM fraction remaining blocked above T2) multiplied by the intensity of the laboratory field. The intensity value for one specimen is finally derived from the average of all  $R'(T_i)$  data between T1 and T2. When the original TRM is affected after T1 by a second small component of magnetization that can be of viscous, chemical or thermal origin, the computation of the  $R'(T_i)$  values is then done between a higher temperature  $T_1'$  and T2.

It is important to note that in the Triaxe protocol we compare NRM and TRM fractions which were acquired in rather similar conditions – from the Curie temperature ( $T_c$ ) to T1 in the case of the NRM and from a high temperature T2 close to  $T_c$  down to T1 for the TRM. For this reason, biases due to the presence of multi domain grains, if any, should not significantly affect our intensity determinations.

In this protocol, the laboratory field is applied in the same direction to that of the NRM and adjusted, when the anisotropy is too strong, to always produce a TRM almost parallel to the NRM. The intensity values obtained using the Triaxe are thus corrected for the TRM anisotropy effect and it was also shown experimentally that they also take into account the cooling rate dependence of the NRM-TRM (Le Goff and Gallet, 2004). Once a sample is loaded, the Triaxe protocol therefore allows us to automatically perform the entire set of intensity measurements in about 2 h. This saves the operator a large amount of time compared to more classical protocols using magnetization measurements at ambient temperature after each heating step. The selection criteria considered in this study are those previously defined by Gallet and Le Goff (2006) and are summarized in Table 2 in the Appendix.

## 4. Results

Eleven groups of four to seven fragments were studied using the TT-IZZI intensity procedure. The intensity determinations for the fragments that fulfill our selection criteria are reported in Table 3 in the Appendix (Fig. 5). The rate of success is  $\sim 55\%$ . The fragments were mainly rejected due to the detection of a high level of alteration of the magnetic mineralogy, because of non-linear Arai diagrams, complex thermal demagnetization diagrams and because of the non-coherence of intensity results obtained at the fragment level. Applying our additional criterion relative to the comparison between the IZ and ZI steps leads to the rejection of 11 fragments previously retained in Gallet et al. (2005) and the present paper therefore updates the data of 2005 (Table 3 in the Appendix).

Thirty two fragments were the subject of a dual intensity determination using the TT-IZZI and the Triaxe protocol. Thirteen

other fragments previously studied by Genevey and Gallet (2002) using the Thellier and Thellier method as modified by Aitken (e.g. 1998), i.e. TT-IZ protocol, were also re-analyzed using the Triaxe. Note that it was not possible to perform a systematic comparison for all fragments successfully analyzed using either the TT-IZZI or the TT-IZ protocol because the magnetization of some of them was not strong enough to be measured with the Triaxe magnetometer. This is, in particular, the case for all fragments from group A32 (Genevey and Gallet, 2002), which are thus not re-analyzed in the present paper.

As previously reported for Syrian fragments (Gallet and Le Goff, 2006), very good agreement between intensity determinations obtained using classical Thellier and Thellier protocols (TT-IZZI or TT-IZ) and the Triaxe procedure is observed at the fragment level with differences lying within a span of  $\sim 5\%$  for all but seven fragments (Fig. 6a). Among the latter fragments, those from site A18 are the most discrepant yielding always higher intensity values when analyzed on the Triaxe magnetometer. No such systematic deviation is observed for our other sites.

At the site level, we further compared the intensity means derived from respectively the TT-IZZI or TT-IZ and the Triaxe values. The computation was made for each protocol when the number of successful analyzed fragments was greater than three per site (incorporating also the seven discrepant fragments mentioned above). As observed on Fig. 6b, the two means for all sites but A18 are very consistent, with differences of less than  $\pm \sim 5\%$ . For group A18, the discrepancy is of about  $-11.5\%$ . It is interesting to note that its Triaxe intensity mean ( $53.8 \pm 1.2 \mu\text{T}$ ) would be perfectly consistent with several other mean intensity values of similar ages (EC02, LAN01, A22, PAL02, TA01) regardless of the protocol used while its TT-IZ mean ( $48.4 \pm 2.5 \mu\text{T}$ ) would be too low (Table 1). Although we can reasonably suspect that our previous intensity determination with the TT-IZ protocol was underestimated, possibly due to an overestimation of the cooling rate correction, we chose to reject the A18 site on the basis of a negative comparison test between the Triaxe and the TT-IZ protocols.

Excluding the fragments from site A18, we finally compared the intensity values obtained at the fragment level before and after cooling rate correction using the TT-IZZI or TT-IZ protocols with the Triaxe data. The distribution of the differences expressed in percent clearly appears better clustered after the cooling rate correction with a mean shifting from about 5% to about 0%, thus confirming that the Triaxe protocol indeed efficiently takes into account the cooling rate effect (Fig. 6c,d; Le Goff and Gallet, 2004). The reliability of the Triaxe intensity determinations already underlined from the analysis of fragments from the Middle East (Gallet and Le Goff, 2006) is hence further strengthened with this collection of French archeological artifacts, which is very different in terms of the magnetic mineralogy, baking and the conditions of preservation of the fragments.

The Triaxe protocol was thus applied to the analysis of 43 groups of fragments. Between 2 and 10 mini cores were measured per group and the successful intensity determinations obtained (about 70% of success rate) are reported in Table 4 in the Appendix (Fig. 7).

Table 1 summarizes the mean intensity values derived for each group of our collection. It is worth noting that when two protocols were applied on the same fragment, all values obtained at the specimen level were simply averaged to compute the mean intensity value for the fragment. The mean intensity values appear well defined with standard deviations usually less than  $2.5 \mu\text{T}$  ( $\sim 5\%$  of the mean).

When specifically examining the sites for which several archeological units of the same age were analyzed, a very good agreement is observed between the mean values obtained from those units. This is, for example, the case for the MON01, MON07 and MON08 groups, all three associated with the same period of use of kiln #1007 excavated in Montpellier in the so-called Boissier faience workshop (Ginouvez et al., 2001). The very good consistency between the three values obtained from a group of bricks taken from the kiln (MON08) and from two sets of potsherds found directly inside the kiln (MON01 and

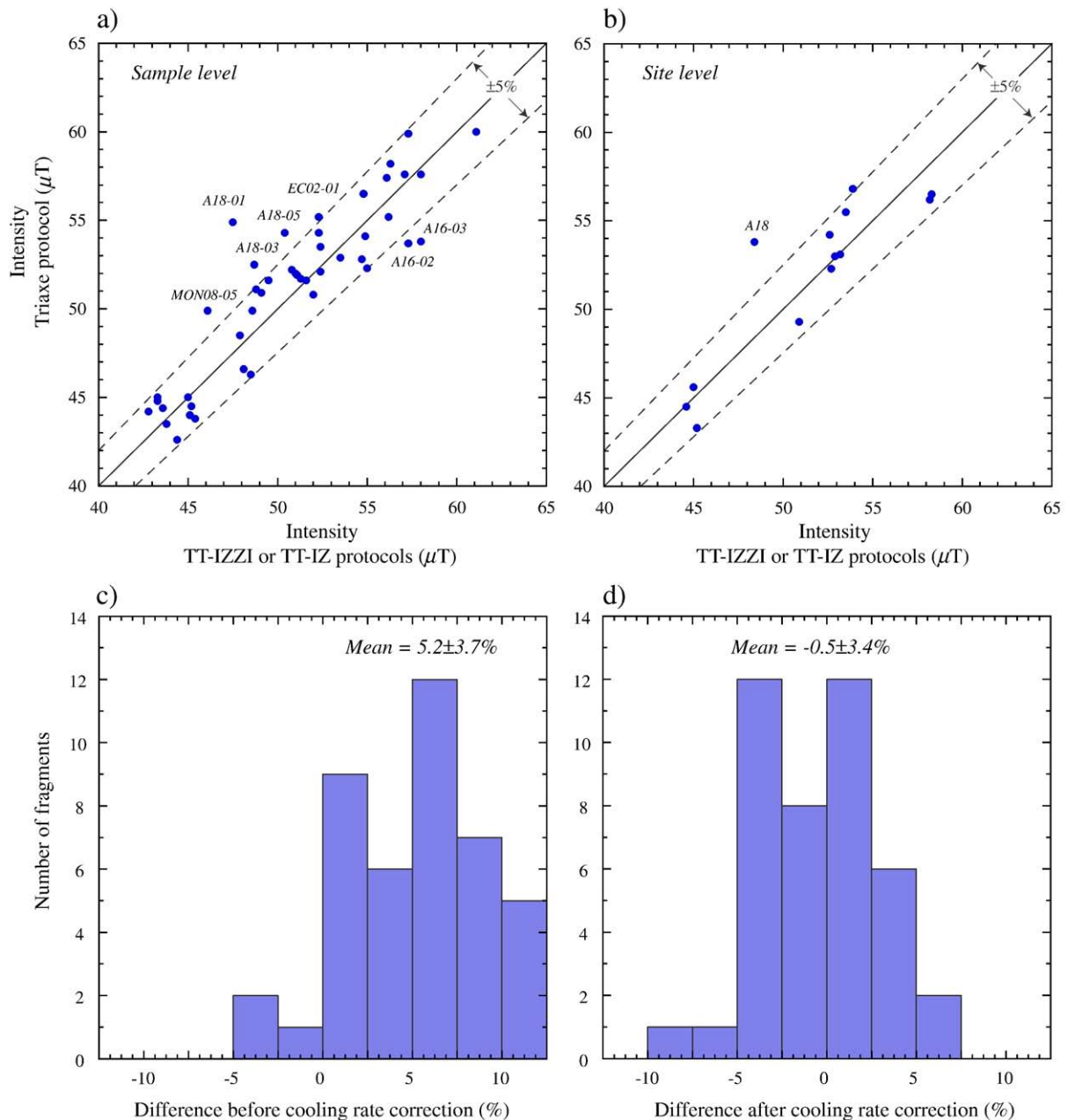


**Fig. 6.** Comparisons between intensity results obtained for specimens from the same fragments using both the TT-IZZI or TT-IZ and the Triaxe protocols. Comparisons performed at the fragment level (a) and at the site level (b). The dashed lines surround the area of agreement at 5%. (c) (resp. d) Histograms of the differences (expressed in %) between the two data sets considering the results derived from the TT-IZZI or TT-IZ protocols before (resp. after) cooling rate correction. Fragments from site A18 were not considered in these histograms. The two mean values are given with their standard deviation.

MON07) allows us to compute with confidence a mean value for this structure. The neighbouring kilns #1003 and #3029 from the same workshop and of the same age were also analyzed and it is satisfactory to observe that the intensity values obtained for the groups of ceramic fragments found inside kiln #1003 (site MON03) and inside kiln #3029 (sites MON04 and MON05) are very consistent with the main value obtained for kiln #1007. A similar agreement is obtained in several other cases: groups LYON01/A, /B, /C associated to the faience workshop of Joseph Combe, groups BDE01 and BDE02 for the Bois d'Epense workshop and groups ART02 and ART03 for the Arthé workshop. A "master" mean intensity value was thus calculated for each of these three main sites.

In all, the different comparisons we made at the fragment, archaeological unit, protocol, and site levels underline the high reliability of the archeointensity data determined from this archeological collection. They

further show that precise and coherent intensity data may be obtained from well dated fragments when an adequate intensity protocol, taking into account the anisotropic nature of the objects analyzed and the cooling rate effect, and strict selection criteria are applied.

## 5. Discussion

Our new mean archeointensity values, together with one data that we previously acquired on French potsherds for the same time period (group A32; Genevey and Gallet, 2002), draw a consistent path for intensity variations in Western Europe over the past 800 years (Fig. 8a). These fluctuations are comparable to those described in Gallet et al. (2005) but are now much better defined. Our new data confirms the existence of two intensity maxima during the second half of the XIVth century and at the end of the XVth century with a smooth increase in

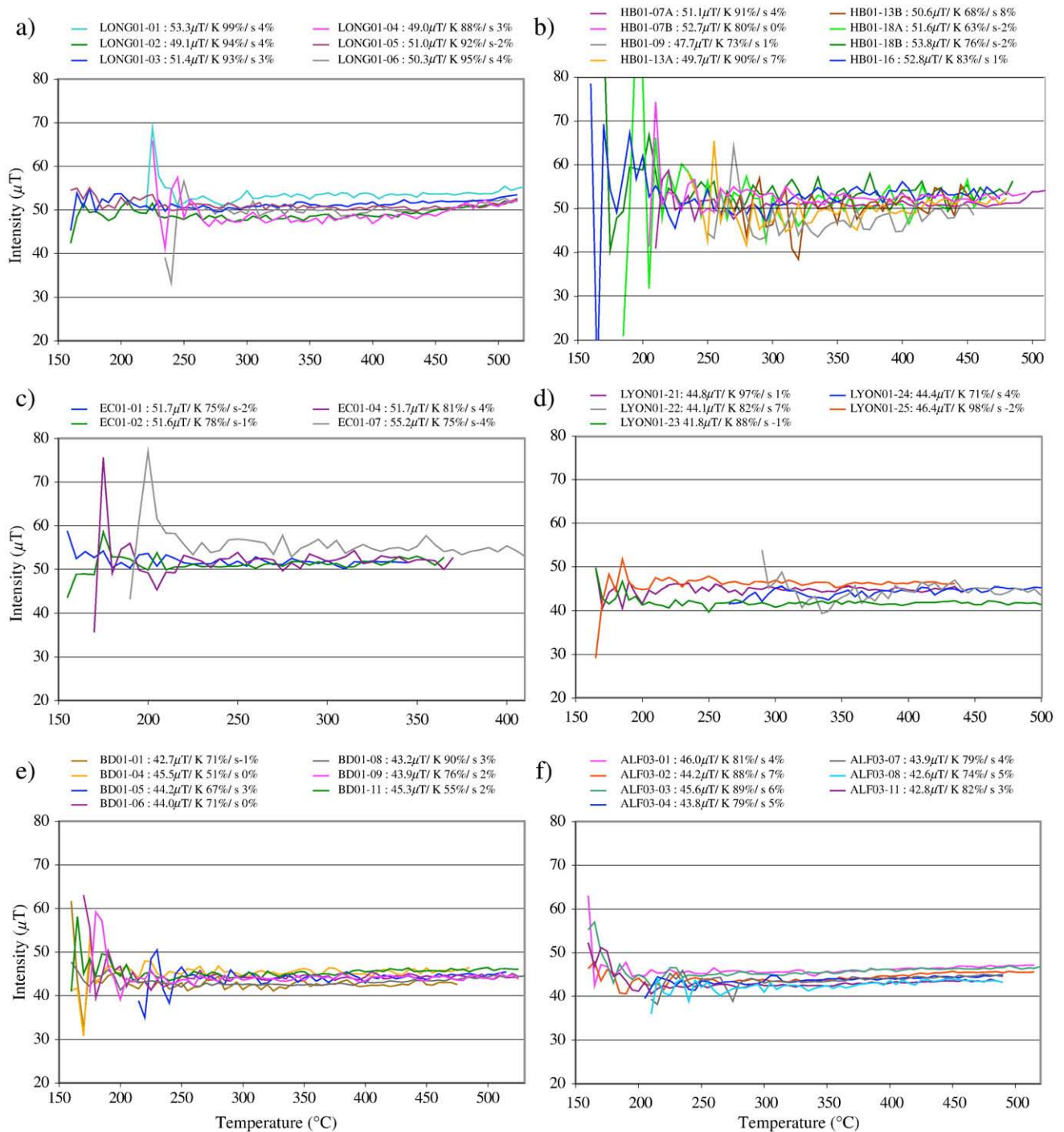


**Fig. 7.** Intensity determinations obtained for 6 groups using the Triaxe protocol. One or sometimes two specimens were analyzed per fragment providing each individual  $R'(Ti)$  curve in the different panels, and each site comprises several fragments ( $\geq 2$ ) (Le Goff and Gallet, 2004; Gallet and Le Goff, 2006). (For interpretation of the references to color in this figure, the reader is referred to the web version of this article.)

intensity during the Renaissance period in France (XVIth century). After the Renaissance, a rapid and important decrease in intensity is observed until the second half of the XVIIIth century with a rate of decrease of  $\sim 7 \mu\text{T}$  per century. Note that this rate is very similar to the one which, according to Genevey and Gallet (2002) prevailed in France between the VIIIth and Xth centuries. After  $\sim 1800$ , the archeointensity values increase smoothly and closely approach the first direct intensity measurements made in the vicinity of Paris at the end of the XIXth century (<http://www.bcmf.fr>).

This coherent dataset includes enough results to allow the construction of a mean curve for France over the past 800 years. We

computed mean intensity values with 50 year sliding windows shifted by 25 years and retained only those defined from at least 3 different data (Fig. 8b). Our resulting curve describes particularly well the three periods of intensity increase previously mentioned. However, well dated data is still required to better document the periods of intensity decrease during the XVth century and from the middle of the XVIth to the middle of the XVIIIth centuries.

We also compared our new data with previously published results from France and nearby countries. For this, we used the ArcheoInt compilation of intensity data for the past 10000 years (Genevey et al., 2008; <http://ArcheoInt.free.fr>) and selected within a box centered around Paris (of  $30^\circ$

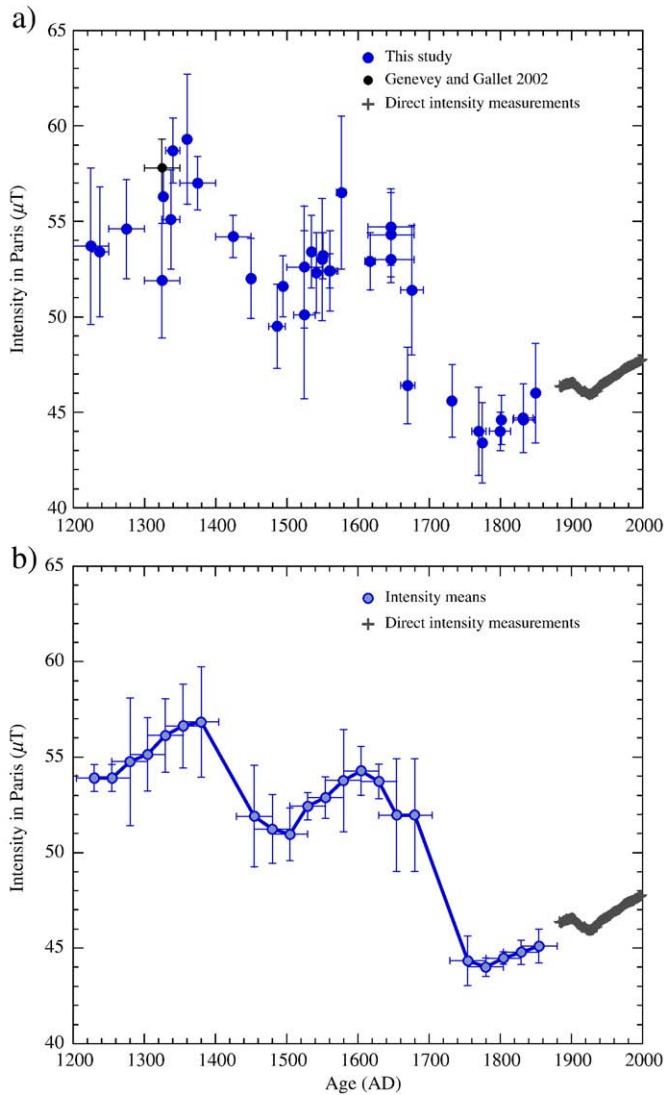


**Fig. 8.** Geomagnetic field intensity variations in Western Europe as deduced from our new archeointensity data and from direct intensity measurements (grey crosses). (a) Individual intensity values obtained per site in this study (blue circles), together with one result previously obtained by Genevey and Gallet (2002; black circle). (b) Intensity averages computed from data from (a) using sliding windows of 50 years shifted every 25 years. (For interpretation of the references to color in this figure, the reader is referred to the web version of this article.)

in both longitude and latitude) only data fulfilling a set of standard basic criteria. These criteria, defined in Genevey et al. (2008) are the following: (1) the data must be acquired using the original or derived Thellier and Thellier method with pTRM-check tests or with the original Shaw procedure, 2) the mean intensity value must be computed from at least three results, regardless of the definition of the site (fragment or group of fragments), 3) the standard deviation must be less than 15%, and 4) the TRM anisotropy effect must be taken into account for objects generally recognized as strongly anisotropic, such as fragments of pottery or tiles.

The data thus selected are from Shaw (1974; England and Italy), Games and Baker (1981; England), Chauvin et al. (2000; France), Gram-Jensen et al. (2000; Denmark and Norway) and Casas et al. (2005, 2007; England). Recently new archeointensity data, now included in the Archeoint compilation, were obtained from Spain by Gómez-Paccard and co-authors (2008) and from Portugal by Hartmann and co-authors (2008). These values were determined using respectively the original Thellier and Thellier method (1959) and the modification of it by Coe (1967) with, in both cases, pTRM-check tests and corrections for TRM anisotropy and cooling rate effects. Two data points from Hartmann et al. (2008) were rejected since these authors suspected a younger re-heating

for one fragment (SC1) and because of a too large dispersion around the mean value obtained for a second potsherd (SC4). The other data from Portugal and from Spain fulfill all of the above selection criteria and are thus also considered in the following. For allowing comparisons between the different selected datasets, all the values were reduced to the latitude of Paris using the hypothesis of an axial dipole field. We further applied a cooling rate correction factor of 5% for the data for which this effect was not taken into account (Genevey and Gallet 2002; Genevey et al., 2008).

All data are reported in Fig. 9a. A first look at this figure shows a large data scatter between 1200 and 1600 when the data is most

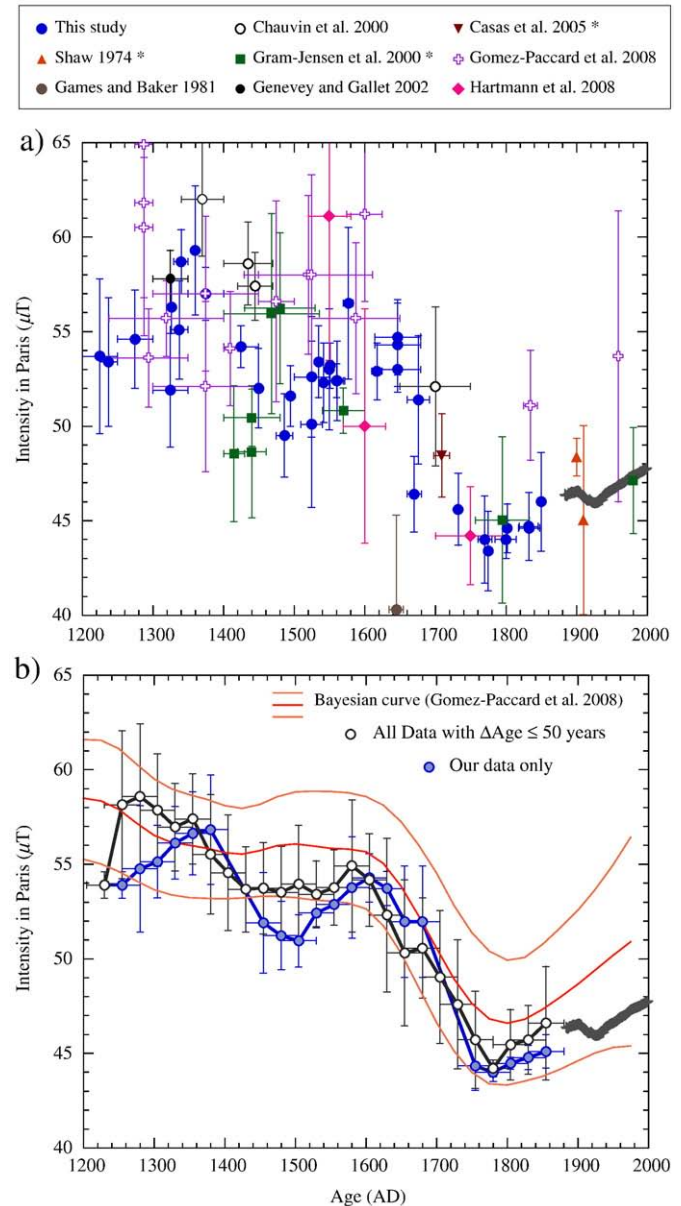


**Fig. 9.** Comparison between our intensity data set and others results previously obtained by several authors for Western Europe and fulfilling a set of standard basic criteria (a) Individual intensity values obtained by Shaw (1974), Games and Baker (1981), Chauvin et al. (2000), Gram-Jensen et al. (2000), Genevey and Gallet (2002), Casas et al. (2005, 2007), Gómez-Paccard et al. (2008), Hartmann et al. (2008) and this study. "\*" indicates the data for which the cooling rate effect was not originally taken into account and for which a correction of 5% decrease was implemented. (b) Comparison between the mean intensity curve derived from our data only (blue circles) and the one computed from all data with age uncertainties less than 100 years (open black circles). In both cases, sliding windows of 50 years shifted every 25 years were used. The curve in orange corresponds to the Bayesian intensity evolution proposed by Gómez-Paccard et al. (2008). (For interpretation of the references to color in this figure, the reader is referred to the web version of this article.)

numerous. A better agreement is observed between the fewer data available between 1600 and 1800 (Games and Baker 1981; Chauvin et al., 2000; Gram-Jensen et al., 2000; Casas et al., 2005, 2007; Gómez-Paccard et al., 2008; Hartmann et al., 2008; this paper), all of them supporting a significant intensity decreasing trend. For the two most recent centuries, the data of Gómez-Paccard et al. (2008) appear too high compared to our data (but the latter are slightly older) and to the geomagnetic field in Paris at 1959 (although the standard deviation found for the 1959 data includes the known value). Two other values obtained by Shaw (1974) are closer to the direct intensity measurements at the relevant dates. An even better agreement is observed for one Danish result at 1980 from Gram-Jensen et al. (2000).

The large dispersion of the data observed between 1200 and 1600 was previously discussed by Gómez-Paccard et al. (2008). From their data, together with other data available from Western Europe for this time interval (Chauvin et al., 2000; Gram-Jensen et al., 2000; Genevey and Gallet, 2002; Gallet et al., 2005), Gómez-Paccard et al. (2008) questioned the occurrence of the two maxima proposed by Gallet et al. (2005). These authors instead suggested a rather flat intensity evolution between the XIIIth and the XVIth century, arguing that the discrepancies observed between intensity values of the same age (for instance at the end of the XIIIth century but see also Gómez-Paccard et al., 2006b) are of course linked to the age uncertainties but also express the limitations of the experimental method and/or of the archeomagnetic record.

Incorporating our new results into the entire data collection and selecting only the data with age uncertainties of less than 100 years, results in the elimination of most of the intensity fluctuations drawn by our own data. In this respect, the curve obtained between AD 1200 and AD 1600 from the scattered data distribution (see Fig. 9a) appears more compatible with the flat evolution proposed by Gómez-Paccard et al. (2008; Fig. 9b). We recognize that the data scatter is very puzzling and clearly raises questions as to the reliability of at least some results. Nevertheless, based on the different reliability tests we present above, we consider that well-dated archeointensity determinations can be accurate enough to reveal rapid fluctuations of the magnetic field and that our new data further support the results of Gallet et al. (2005).

It is worth mentioning that the evolution in geomagnetic field intensity over the past few centuries that we suggest here clearly opens the possibility to use archeointensity (at least over the period considered) as an efficient dating tool for archeological purposes. In particular, such an application of archeomagnetism, generalizing that of the archeomagnetic directional variations, may provide useful dating constraints for detecting fake production of supposedly “old” decorated faïences.

There are no direct intensity measurements prior to the middle of the XIXth century (Barraclough, 1974). To constrain their geomagnetic field models (gufm1), Jackson et al. (2000) used the hypothesis of a constant decrease of the axial dipole moment between 1590 and 1840, extrapolating the known rate observed after 1840 (i.e. 15 nT per year). This trend was recently reconsidered by Gubbins et al. (2006) and Finlay (2008). From the worldwide archeointensity data compilation of Korte et al. (2005), Gubbins et al. (2006) computed for each relevant intensity result a corresponding  $g_1^0$  value relying on the geometry of the gufm1 models. They hence derived a linear evolution for this term prior to 1840 with a rate of only  $2.28 \pm 2.72$  nT per year. A different approach was used by Finlay (2008) who carried out a new inversion of the historical directional observations compiled by Jackson et al. (2000) complemented by the archeointensity data collection of Korte et al. (2005). This author concluded that the most probable model involves no change for the  $g_1^0$  term between 1590 and 1840 (gufm1-g10c model).

Using the original models of Jackson et al. (2000), and those for the period between 1590 and 1840 recalibrated with the nearly constant  $g_1^0$  as found by Gubbins et al. (2006) and Finlay (2008), we computed the corresponding intensity variations curves expected in Paris (Fig. 10a). The resulting curves display similar trends but with different ampli-

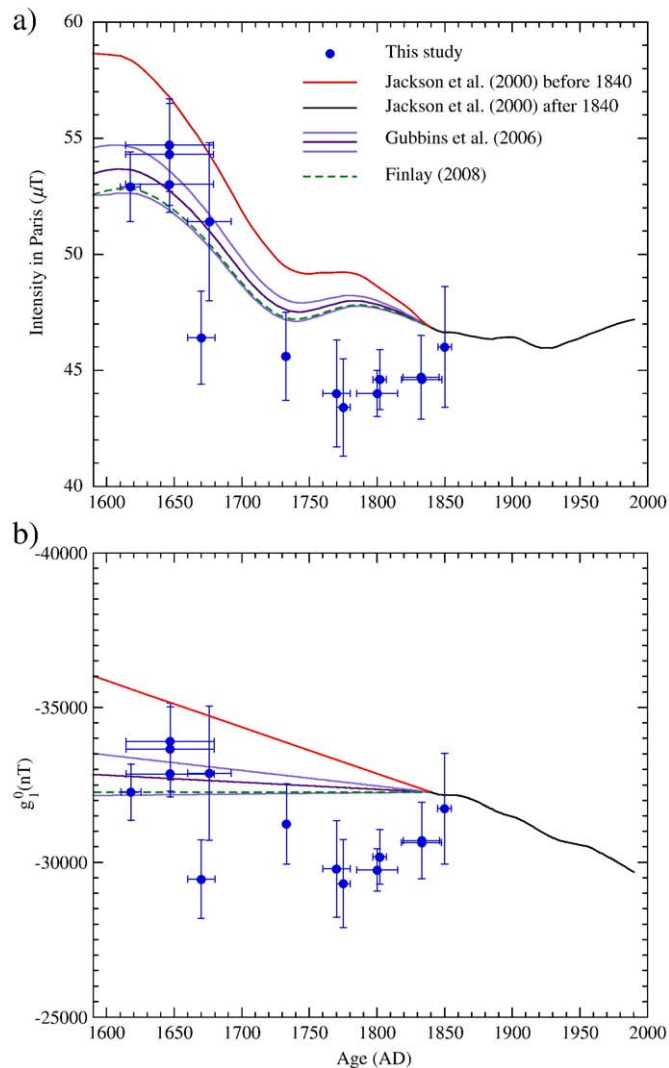


**Fig. 10.** Comparison between our data and different geomagnetic field models available for the period 1590–2000. (a) Comparison between our new intensity data (in blue) and the intensity evolution expected in Paris from the original models of Jackson et al. (2000 - in red before 1840 and in black after), and from the same models recalibrated using the  $g_1^0$  evolution proposed by Gubbins et al. (2006; in purple) and Finlay (2008; in green). (b) Comparison between different evolutions in  $g_1^0$  (same conventions as in Fig. 8a) and the  $g_1^0$  values deduced from our archeointensity data from France considering the geomagnetic field geometry proposed by Jackson et al. (2000). See the text for further details. (For interpretation of the references to color in this figure, the reader is referred to the web version of this article.)

tudes. When comparing them with our mean archeomagnetic curve, good agreement is found for the period ~1590–1700 with the variations deduced from the  $g_1^0$  evolution of Gubbins et al. (2006) and also of Finlay (2008). However after ~1700, our intensity results appear lower by ~3 to 4  $\mu\text{T}$  to the predicted values. It is worth pointing out that what was first suspected from a limited data set (Gallet et al., 2005), namely a time interval with relative low intensities between ~1730 and ~1840 is confirmed by our new data. The fact that the data is truly independent, i.e. the artifacts come from different contexts and different places (different clay deposits, various manufacturing conditions, etc.), and the consistency between our data set obtained from two different protocols clearly make a systematic error or bias very unlikely (as suggested by Finlay, 2008 to explain the differences observed between his models and the data reported by Gallet et al., 2005). Using our own data collection and following the same approach as Gubbins et al. (2006), we then computed the temporal evolution of the “recalibrated”  $g_1^0$  term (Fig. 10b). In contrast with previous studies (Jackson et al., 2000; Gubbins et al., 2006; Finlay, 2008), our results clearly tend to favor a

non-linear evolution of the axial dipole term between 1590 and 1850. This evolution seems to be characterized initially by a decrease between 1590 and ~1780, then by a (moderate) increase until ~1850 and finally by the well- documented decrease up to the present day. At this stage, the revised evolution in  $g_1^0$  that we propose here calls for additional well-dated reliable archeointensity data. It further shows the crucial need to reduce the scatter in the regional data sets presently available.

## Acknowledgments

We especially wish to thank the following archeologists, historians and museum curators for providing the fragments and for their time and generous help: P. André, C. Becker, R. and S. Biton, G. Blanc, A. L. Bugnon, K. Degroote, J.-P. Delor, B. François, R. Guadagnin, A. Horry, J. Jouët, A. Kauffmann, A. Le Bot Helly, O. Leconte, H. Martin, C. Pellet, F. Ravoire, R. de Saint-Seine, N. Thomas, J. Thiriot, A. Vaillant, L. Vallauri, J.-L. Vayssettes. We also would like to thank Gauthier Hulot, Vincent Courtillot and Ruven Pillay for their help in improving the manuscript. We further thank Rob Coe and an anonymous reviewer who made helpful comments on the paper. This study was partly financed by the INSU-CNRS program "SEdit". This is IGP contribution no. 2506.

## Appendix A. Supplementary data

Supplementary data associated with this article can be found, in the online version, at [doi:10.1016/j.epsl.2009.04.024](https://doi.org/10.1016/j.epsl.2009.04.024).

## References

- Aitken, M.J., Alcock, P.A., Bussell, G.D., Shaw, C.J., 1981. Archaeomagnetic determination of the past geomagnetic intensity using ancient ceramics: allowance for anisotropy. *Archaeometry* 23, 53–64.
- Aitken, M.J., Allsop, A.L., Bussell, G.D., Winter, M.B., 1988. Determination of the intensity of the Earth's magnetic field during archaeological times: reliability of the Thellier technique. *Rev. Geophys.* 26, 3–12.
- Barraclough, D., 1974. Spherical harmonic analysis of the geomagnetic field for eight epochs between 1600 and 1910. *Geophys. J. R. Astron. Soc.* 43, 497–513.
- Bucur, I., 1994. The direction of the terrestrial magnetic field in France during the last 21 centuries. *Phys. Earth Planet. Inter.* 87, 95–109.
- Casas, L., Shaw, J., Gich, M., Share, J.A., 2005. High-quality microwave archaeointensity determinations from an early 18th century AD English brick kiln. *Geophys. J. Int.* 161, 653–661.
- Casas, L., Linford, P., Shaw, J., 2007. Archaeomagnetic dating of Dogmersfield Park brick kiln (Southern England). *J. Archaeol. Sci.* 34, 205–213.
- Chauvin, A., Garcia, Y., Lanos, P., Laubenheimer, F., 2000. Paleointensity of the geomagnetic field recovered on archaeomagnetic sites from France. *Phys. Earth Planet. Inter.* 120, 111–136.
- Coe, R., 1967. Paleo-Intensities of the Earth's magnetic field determined from Tertiary and Quaternary Rocks. *J. Geophys. Res.* 72, 3247–3262.
- Coe, R., Grommé, S., Mankinen, E., 1978. Geomagnetic paleointensities from radio-carbonated lava flows on Hawaii and the question of the Pacific nondipole low. *J. Geophys. Res.* 83, 1740–1756.
- Day, R., Fuller, M., Schmidt, V., 1977. Hysteresis properties of titanomagnetites: Grain size and composition dependence. *Phys. Earth Planet. Inter.* 13, 260–267.
- Finlay, C.C., 2008. Historical variation of the geomagnetic axial dipole. *Phys. Earth Planet. Inter.* 170, 1–14. [doi:10.1016/j.pepi.2008.06.029](https://doi.org/10.1016/j.pepi.2008.06.029).
- Gallet, Y., Le Goff, M., 2006. High-temperature archeointensity measurements from Mesopotamia. *Earth Planet. Sci. Lett.* 241, 159–173.
- Gallet, Y., Genevey, A., Le Goff, M., 2002. Three millennia of directional variation of the Earth's magnetic field in western Europe as revealed by archaeological artefacts. *Phys. Earth Planet. Inter.* 131, 81–89.
- Gallet, Y., Genevey, A., Fluteau, F., 2005. Does Earth's magnetic field secular variation control centennial climate change? *Earth Planet. Sci. Lett.* 236, 339–347.
- Gallet, Y., Genevey, A., Le Goff, M., Fluteau, F., Eshraghi, S.A., 2006. Possible impact of the Earth's magnetic field on the history of ancient civilizations. *Earth Planet. Sci. Lett.* 246, 17–26.
- Gallet, Y., Hulot, G., Chulliat, A., Genevey, A., in press. Geomagnetic field hemispheric asymmetry and archeomagnetic jerks. *Earth Planet. Sci. Lett.* [doi:10.1016/j.epsl.2009.04.028](https://doi.org/10.1016/j.epsl.2009.04.028).
- Games, K.P., Baker, M.E., 1981. Determination of geomagnetic archaeomagnitudes from clay pipes. *Nature* 289, 478–479.
- Genevey, A., Gallet, Y., 2002. Intensity of the geomagnetic field in western Europe over the past 2000 years: new data from ancient French pottery. *J. Geophys. Res.* 107 (B11). [doi:10.1029/2001JB000701](https://doi.org/10.1029/2001JB000701).
- Genevey, A., Gallet, Y., Constable, C.G., Korte, M., Hulot, G., 2008. ArcheoInt: An upgraded compilation of geomagnetic field intensity data for the past ten millennia and its application to the recovery of the past dipole moment. *Geochem Geophys Geosyst.* 9, Q04038. [doi:10.1029/2007GC001881](https://doi.org/10.1029/2007GC001881).
- Ginouvez, O., Fabre, L., Forest, V., Foy, D., Henry, E., Leenhardt, M., Thiriot, J., Vallauri, L., Vayssettes, J.-L., 2001. Montpellier (34) Tramway: Pôle d'Echange Corum, Fenêtre sur le Faubourg du Pila-Saint-Gely (XIV–XXe siècle). Faïencerie Favier (XVIIIe siècle), DFS de fouille préventive (13–24 décembre 1999/13 mars–30 mars 2000) AFAN, Aix-en-Provence, Laboratoire d'Archéologie Médiévale Méditerranéenne.
- Gómez-Paccard, M., Catanzariti, G., Ruiz-Martínez, V.C., McIntosh, G., Núñez, J.L., Osete, M.L., Chauvin, A., Lanos, P., Tarling, D.H., Bernal-Casasola, D., Thiriot, J., 2006a. A catalogue of Spanish archeomagnetic data. *Geophys. J. Int.* 166, 1125–1143.
- Gómez-Paccard, M., Chauvin, A., Lanos, P., Thiriot, J., Jiménez-Castillo, P., 2006b. Archeomagnetic study of seven contemporaneous kilns from Murcia (Spain). *Phys. Earth Planet. Inter.* 157 (1–2), 16–32. [doi:10.1016/j.pepi.2006.03.001](https://doi.org/10.1016/j.pepi.2006.03.001).
- Gómez-Paccard, M., Chauvin, A., Lanos, P., Thiriot, J., 2008. New archeointensity data from Spain and the geomagnetic dipole moment in western Europe over the past 2000 years. *J. Geophys. Res.* 113, B09103. [doi:10.1029/2008JB005582](https://doi.org/10.1029/2008JB005582).
- Gram-Jensen, M., Abrahamson, N., Chauvin, A., 2000. Archaeomagnetic intensity in Denmark. *Phys. Chem. Earth* 25, 525–531.
- Gubbins, D., Jones, A.L., Finlay, C.C., 2006. Fall in Earth's Magnetic Field Is Erratic. *Science* 312, 900–902.
- Hartmann, G.A., Trindade, R.I.F., Goguitchaichvili, A., Etchevarne, C., Morales, J., Afonso, M.C., 2008. First archeointensity results from Portuguese potteries (1550–1750 AD). *Earth Planets Space* 61, 93–100.
- Jackson, A., Jonkers, A., Walker, M., 2000. Four centuries of geomagnetic secular variation from historical records. *Philos. Trans. R. Soc. Lond. Ser. A* 358, 957–990.
- Korte, M., Genevey, A., Constable, C.G., Frank, U., Schnepp, E., 2005. Continuous geomagnetic models for the past 7 millennia I: a new global data compilation. *Geochem. Geophys. Geosyst.* 6 (2), Q02H15. [doi:10.1029/2004GC000800](https://doi.org/10.1029/2004GC000800).
- Lanos, P., Kovacheva, M., Chauvin, A., 1999. Archaeomagnetism, methodology and application: implementation and practice of the archaeomagnetic method in France and Bulgaria. *Eur. J. Archaeol.* 2, 365–392.
- Le Goff, M., Gallet, Y., 2004. A new three-axis vibrating sample magnetometer for continuous high-temperature magnetization measurements: applications to paleo- and archeo-intensity determinations. *Earth Planet. Sci. Lett.* 229, 31–43.
- Le Goff, M., Gallet, Y., Genevey, A., Warmé, N., 2002. On archaeomagnetic secular variation curves and archaeomagnetic dating. *Phys. Earth Planet. Inter.* 134, 203–211.
- Marchesi, H., Thiriot, J., Vallauri, L., 1997. Marseille, les ateliers de potiers du XIIIe s. et le quartier Sainte-Barbe (Ve–XVIIe s.). Documents d'Archéologie Française n°65, Editions de la Maison des sciences de l'homme.
- Nagata, T., Arai, Y., Momose, K., 1963. Secular variation of the geomagnetic total force during the last 5000 years. *J. Geophys. Res.* 68, 5277–5281.
- Rogers, J., Fox, J., Aitken, M., 1979. Magnetic anisotropy in ancient pottery. *Nature* 277, 644–646.
- Rosen, J., 2000. La faïence française du XIIIe au XVIIe siècle. Dossier de l'Art 70.
- Rosen, J., 2001. (dir.) Faïenceries françaises du Grand Est: inventaire Bourgogne–Champagne–Ardenne (XIVe–XIXe s.). CTHS, Paris.
- Rose, J., Crépin-Leblond, T., (dir.) 2000. Images du pouvoir: les pavements de faïence en France du XIIIe au XVIIe siècle. préface de Michel Pastoureau, Paris-Lyon, Réunion des Musées Nationaux/Bourg-en-Bresse, Musée de Brou.
- Selkin, P.A., Tauxe, L., 2000. Long-term variations in paleointensity. *Phil. Trans. R. Soc. Lond. Ser. A* 358, 1065–1088.
- Shaw, J., 1974. A new method of determining the magnitude of the palaeomagnetic field: Application to five historic lavas and five archaeological samples. *Geophys. J. R. Astron. Soc.* 39, 133–141.
- Tema, E., Hedley, I., Lanos, P., 2006. Archeomagnetism in Italy: a compilation of data including new results and a preliminary Italian secular variation curve. *Geophys. J. Int.* 167, 1160–1171.
- Thellier, E., 1981. Sur la direction du champ magnétique terrestre en France durant les deux derniers millénaires. *Phys. Earth Planet. Inter.* 24, 89–132.
- Thellier, E., Thellier, O., 1959. Sur l'intensité du champ magnétique terrestre dans le passé historique et géologique. *Ann. Géophys.* 15, 285–376.
- Usoskin, I., Korte, M., Kovaltsov, G., 2008. Role of centennial geomagnetic changes in local atmospheric ionization. *Geophys. Res. Lett.* 35, L05811. [doi:10.1029/2007GL033040](https://doi.org/10.1029/2007GL033040).
- Veitch, R., Hedley, I., Wagner, J.-J., 1984. An investigation of the intensity of the geomagnetic field during Roman times using magnetically anisotropic bricks and tiles. *Arch. Sci. (Geneva)* 37, 359–373.
- Warmé, N., 2005. La datation des structures de combustion par la méthode archéomagnétique: quelques exemples normands. actes du 10ème congrès des sociétés historiques et archéologiques de Normandie. Annales de Normandie, pp. 57–61.
- Yu, Y., Tauxe, L., Genevey, A., 2004. Toward an optimal geomagnetic field intensity determination technique. *Geochem. Geophys. Geosyst.* 5, Q02H07. [doi:10.1029/2003GC000630](https://doi.org/10.1029/2003GC000630).
- Zanani, I., Batt, C.M., Lanos, P., Tarling, D.H., Linford, P., 2007. Archaeomagnetic secular variation in the UK during the past 4000 years and its application to archaeomagnetic dating. *Phys. Earth Planet. Inter.* 160, 97–107.